

Received Date : 27-Jan-2014

Revised Date : 25-Mar-2014

Accepted Date : 27-Mar-2014

Article type : Original Research

## **Dynamics of microvascular blood flow and oxygenation measured simultaneously in human skin**

Katarzyna Z Kuliga<sup>1</sup>, Erin F McDonald<sup>1</sup>, Rodney Gush<sup>3\*</sup>, C Charles Michel<sup>4</sup>, Andrew J. Chipperfield<sup>2</sup>, Geraldine F. Clough<sup>1</sup>

<sup>1</sup>Human Development & Health, Faculty of Medicine, University of Southampton, UK

<sup>2</sup>Faculty of Engineering Sciences, University of Southampton, UK

<sup>3</sup>Moor Instruments Ltd., Axminster UK, <sup>4</sup> Department of Bioengineering, Imperial College London, London, UK

**Running title:** Skin microvascular blood flow and oxygenation

**Total Number of words in paper excluding refs and figure legends:** 5450

### **Corresponding author:**

Geraldine Clough BSc PhD

Institute of Developmental Sciences

Faculty of Medicine, University of Southampton

Southampton General Hospital (MP 887)

Southampton SO16 6YD. UK

Email g.f.clough@soton.ac.uk

This article has been accepted for publication and undergone full peer review but has not been through the copyediting, typesetting, pagination and proofreading process, which may lead to differences between this version and the Version of Record. Please cite this article as doi: 10.1111/micc.12136

This article is protected by copyright. All rights reserved.

## Abstract

We have evaluated the dynamics of skin microvascular blood flow (BF) and tissue oxygenation parameters (OXY) measured simultaneously at the same site using a combined non-invasive BF+OXY+temperature probe. Skin BF, oxygenated (oxyHb) and deoxygenated (deoxyHb) haemoglobin and mean oxygen saturation (SO<sub>2</sub>) were measured in 50 healthy volunteers at rest and during perturbation of local blood flow by post-occlusive reactive hyperaemia, sympathetic nervous system-mediated vasoconstriction (deep inspiratory breath-hold) and local skin warming. The relationship between BF and SO<sub>2</sub> over the range of flows investigated was described by a non-linear equation with an asymptote for SO<sub>2</sub> of 84% at BF >50 PU. SO<sub>2</sub> was independently associated with BF, skin temperature, BMI and age, which together identified 59% of the variance in SO<sub>2</sub> (p<0.0001). Fourier analysis revealed periodic low frequency fluctuations in both BF and SO<sub>2</sub>, attributable to endothelial (~0.01 Hz), neurogenic (~0.04 Hz) and myogenic (~0.1Hz) flow motion activity. The frequency coherence between the BF and SO<sub>2</sub> signals was greatest in the endothelial and neurogenic frequency bands. The simultaneous evaluation of microvascular blood flow and oxygenation kinetics in healthy skin provides a platform from which to investigate microvascular impairment in the skin and more generally the pathogenesis of microvascular disease.

**Keywords:** skin, microcirculation, laser Doppler flowmetry, white light spectrometry, tissue oxygenation, flow motion, endothelial function

## Abbreviations

BF, Blood flux; DCS, diffuse correlation spectroscopy; IBH, Inspiratory breath-hold; LDF, Laser Doppler flowmetry; NIRS, Near-infrared spectroscopy; OXY, Tissue oxygenation parameters (oxyHb, deoxyHb, totalHb oxygenated, deoxygenated and total haemoglobin); PORH, post occlusive reactive hyperaemia; pO<sub>2</sub>, Partial oxygen pressure; PSD, Power spectral density; RBC, Red blood cells; SO<sub>2</sub>, Tissue oxygen saturation; tcpO<sub>2</sub>, Transcutaneous oxygen partial pressure.

## Introduction

The non-invasive assessment of skin microvascular blood flow has been widely used in both research and in clinical practice to evaluate microvascular impairment and the impact of cardiovascular disease (CVD) risk factors on vascular health (for review see 41). Furthermore, microvascular (dys)function in the skin may serve as a surrogate measure of that in less accessible tissues (18,42) and so provide an early and prognostic indicator of micro- and macro-vascular disease risk and pathogenesis (15,50).

Laser Doppler flowmetry (LDF) is a well-established technique for the non-invasive assessment of skin microvascular blood flow. The measurement is based on red blood cell (RBC) flux expressed in arbitrary 'perfusion units' (PU) and defined as the product of RBC concentration (blood volume) and RBC velocity (7,34). LDF has been used in conjunction with a wide variety of reactivity tests to provide an overall assessment of microvascular health and to explore the mechanisms underlying the regulation of local tissue perfusion (14,26,33,36,41,49).

Tissue oxygen saturation represents a dynamic balance between  $O_2$  supply and  $O_2$  consumption in the capillary, arteriolar and venular beds. Optical technologies that measure haemoglobin oxygen saturation include pulse oximetry, near-infrared spectroscopy (NIRS) and white-light reflectance spectroscopy. NIRS has been used primarily as a research tool to measure haemoglobin oxygen saturation and regional oxygen saturation (for recent reviews see 6 and 21) and indirectly to quantify local blood flow using exogenous tracers or venous occlusion plethysmography (17) in tissues such as muscle, brain and connective tissue. More recently, NIRS has been used in combination with diffuse correlation spectroscopy (DCS) to evaluate haemodynamic and metabolic parameters in exercising skeletal muscle (24,45). As NIR light when applied to the surface of the body must first pass through the skin, the NIRS signal is derived from skin and subcutaneous vascular beds as well as that of the deeper tissues (16). By contrast, white-light reflectance spectroscopy which is similarly based on the Beer-Lambert law measures differences in tissue haemoglobin concentrations in the absorption spectra of the two chromophores - oxygenated and deoxygenated haemoglobin within the visible light spectrum (500 – 650 nm range) (32). As the measurement depth is limited, the white light spectroscopy signal from the skin will be derived largely from the

microvasculature of the upper dermal plexus (2). When combined with LDF, white-light reflectance spectroscopy affords a non-invasive optical tool by which to evaluate haemodynamic and metabolic parameters in the skin.

Spectral analysis of the component frequencies of the LDF signal reveals periodic oscillations in blood flux, which have been shown to reflect the influence of endothelial activity (0.0095 – 0.02 Hz), sympathetic activity (0.02 – 0.06 Hz), myogenic activity in the vessel wall (0.06 – 0.15Hz), respiration (0.15 – 0.4 Hz) and heart beat (0.4 – 1.6 Hz) on local tissue perfusion (27,29,45). Variations in the amplitudes of the low frequency oscillations have been used to explore dysfunction in local control of microvascular perfusion in a wide range of physiological and pathophysiological conditions (20,28,39,40). Whilst changes in LDF attributable to flowmotion have been well described using frequency domain analysis, the frequency components of tissue oxygenation parameters (OXY) either individually or in combination with those of blood flux (LDF) within the microvasculature have yet to be fully elucidated (52). The recent combination of LDF and OXY sensors into a modular system enables the simultaneous measurement of microvascular blood flow, oxygenated haemoglobin (oxyHb), deoxygenated haemoglobin (deoxyHb), total haemoglobin (totalHb) and tissue oxygen saturation ( $SO_2$ ) at the same tissue site and investigation of the oscillatory components of the blood flow and tissue oxygenation signals and their coherence.

The primary objective of our study was to determine the temporal relationship between the BF and OXY signals measured at the same skin site, at rest and during perturbations in microvascular perfusion using a combined laser Doppler and tissue oxygenation probe. We also explored whether the outputs from the combined probe (oxyHb, deoxyHb, totalHb,  $SO_2$ , BF and temperature) could be used as an indicator of tissue status; to understand better the mechanisms underlying the local and systemic regulation of microvascular perfusion; and to test the assumptions around the relationship between microvascular blood flow and tissue oxygenation and oxygen utilization in skin.

## **Materials and Methods**

### **Ethical Approval**

The study was approved by Research Ethics Committee of University of Southampton and Southampton General Hospital (RHMMED0992). The study was performed in accordance with standards set by the Declaration of Helsinki. All participants gave written informed consent.

### **Study design**

Fifty healthy volunteers (24 male; 26 female) mean age  $29.2 \pm 8.1$  y and BMI  $24.3 \pm 3.2$  kg.m<sup>-2</sup> (mean  $\pm$  SD) participated in the study. All participants were non-smokers and refrained from caffeine-containing drinks and food for at least 2 hours and strenuous exercise for 24 hours, before testing. Participants taking medication that could affect skin blood flow reactivity were excluded from the study.

Studies were performed in a temperature-controlled room maintained at between 22-23°C. All participants were acclimatised for 30 min prior to testing. The mean resting forearm skin temperature measured during baseline recording was  $29.4 \pm 2.1$ °C. Measurements were made with the participant sitting comfortably with their arm supported at heart level.

### **Laser Doppler and SO<sub>2</sub> measurements**

Skin blood flux, tissue oxygen saturation and temperature were measured using a combined laser Doppler (LD) and white light reflectance probe (moorCP1T-1000, Moor Instruments Ltd, Axminster, UK) with an LD fibre separation of 0.5 mm and SO<sub>2</sub> separation of 1 mm, using a single point 785 nm, 1 mW low power red laser light source (moorVMS-LDF2, Moor Instruments Ltd, UK) and a 400-700 nm, <6 mW white light source (moorVMS-OXY, Moor Instruments Ltd, UK). The probe was placed on the ventral surface of the non-dominant forearm arm using a double-sided sticky O-ring, approximately 10 cm from the wrist and avoiding visible veins.

Resting BF and OXY parameters were recorded continuously for 10 min prior to perturbation of skin blood flow by (i) post occlusive reactive hyperaemia (PORH) using a pressure cuff placed around upper limb automatically inflated to 180 mmHg for 3 min (moorVMS-PRES, Moor Instruments Ltd, Axminster UK) (13) (ii) transient sympathetic nervous system-mediated vasoconstriction to deep inspiratory breath hold (3 x 6 sec) (29); and (iii) at a site warmed to 43°C for 20 min using a thermostatically controlled heating block (10 mm diameter) (2). Not all perturbations were performed in all individuals in order to avoid possible interaction between the test perturbations.

To test the reproducibility and repeatability of the measurement of BF and OXY using the combined probe, repeated measurements were made in a sub-set of 10 participants at two adjacent sites and at the same site, on two consecutive days. The site and the direction of the probe were marked with a waterproof pen to allow re-alignment of the probe on the following day.

#### **Data analysis**

BF was recorded in arbitrary perfusion units (PU) and  $SO_2$  in per cent (%) derived from measures of oxygenated (oxyHb), deoxygenated haemoglobin (deoxyHb) and total haemoglobin (totalHb) (all expressed in arbitrary units AU) where  $totalHb = oxyHb + deoxyHb$  and  $SO_2 = (oxyHb/totalHb) \times 100 \%$ .

Signals were recorded using a 40 Hz sampling rate. Time-domain analysis was performed in moorVMS-PC software (Moor Instruments Ltd, UK) and MATLAB (R2012a, MathWorks, UK). Values for BF and  $SO_2$  were determined at baseline as a mean value over the final 5 min before perturbation; during the 3 min of arterial occlusion; peak value after release of the cuff; minimum value over the last 3 sec IBH expressed as mean minimum response to the three breath holds ( $IBH_{min}$ ); and mean maximum value over 3 min at the end of tissue warming (43°C, 20 min).

Frequency-domain analysis was performed in MATLAB (R2012a, MathWorks, UK). Prior to spectral analysis, we assessed all traces visually for the presence of artefacts and excluded poor quality recordings. Signals were resampled to 10 Hz and detrended using moving-average with 200s window to remove frequency content below 0.005Hz. Spectral density

was estimated by Welch's method of Fourier transform with a Hanning window size of 200s and 50% overlap between windows using continuous 10 min baseline recordings. The power contribution was evaluated within the frequency range (0.0095-1.6 Hz) divided into frequency intervals corresponding to endothelial activity (0.0095 – 0.02 Hz), sympathetic activity (0.02 – 0.06 Hz), myogenic activity in the vessel wall (0.06 – 0.15Hz), respiration (0.15 – 0.4 Hz) and heart beat (0.4 – 1.6 Hz) (29,47). The absolute spectral power is expressed in  $\text{PU}^2$ . Power spectral density contribution (PSD contribution) was calculated relative to total spectral power and is expressed as a fraction between 0 and 1.

A frequency coherence function describing the linear relationship between two signals in the frequency domain was calculated as ratio between the cross power spectral density and power spectral densities (Eq.1)

$$C_{xy}(f) = \frac{|P_{xy}(f)|^2}{P_{xx}(f)P_{yy}(f)} \quad (1)$$

where  $C_{xy}(f)$  is the coherence between the input signals  $x$  and  $y$ ,  $P_{xy}(f)$  is the cross power spectral density at a given frequency,  $P_{xx}(f)$  and  $P_{yy}(f)$  are the power spectral densities of  $x$  and  $y$  signals at chosen frequency (36). The frequency coherence function  $C_{xy}(f)$  returns a value between 0 and 1, with 1 indicating the same frequency-power characteristics between studied signals (12,35,46).

### Statistical analysis

Statistical analysis was performed using GraphPad Prism (Prism 6, GraphPad Software, Inc., USA) and IBM SPSS Statistics 19 (IBM United Kingdom Limited, UK). Results were considered as significant with  $p < 0.05$ . Data were tested for normal distribution using D'Agostino & Pearson omnibus normality test. Data are presented as either mean  $\pm$  standard deviation (SD) for normally distributed data or median with interquartile range for non-normally distributed data. Normally distributed data were compared using Students t-test and non-normally distributed data using a Mann-Whitney test. Pearson correlation coefficients are presented for univariate regression analysis of baseline data. Multivariable linear regression

Accepted Article

modelling, with resting  $SO_2$  as the dependent (out-come) variable was used to describe factors that were independently associated with  $SO_2$ . Factors that were entered into the regression model as explanatory variables were chosen from the results of the univariate analysis and included resting BF, skin temperature, BMI and age. In all cases a value of  $p < 0.05$  was taken to indicate statistical significance.

Reproducibility of measurements was expressed as inter- and intra-individual coefficients of variation (CV) and repeatability of measurements as intra-class correlation coefficients (ICC) (5). CV values of  $<0.35$  were deemed as acceptable (42) and ICC values of 0.61-0.81 as substantial and 0.81 -1 .00 as almost perfect (51).

## Results

### Reproducibility and repeatability of the combined sensor

The inter-individual CV for resting BF and  $SO_2$  measured using the combined probe was 0.15 and 0.09, respectively ( $n=10$ ). The intra-individual CV for BF and  $SO_2$  measured at the same site on two consecutive days was 0.20 and 0.07, respectively. The intra-individual CV was for skin temperature was 0.009. The inter-individual CVs for oxyHb, deoxyHb and totalHb were 0.19, 0.09 and 0.10, respectively ( $n=10$ ). The inter-individual CV for skin temperature was 0.007 ( $n=10$ ).

The intra-class correlation coefficient (ICC) for resting BF and  $SO_2$  was 0.85 (almost perfect) and 0.68 (substantial), respectively ( $n=10$ ).

### Skin blood flux and oxygenation measured in the time domain using the combined probe

An example of the raw BF and OXY outputs from the combined probe is shown in Figure 1. Values for BF and OXY parameters measured at rest and during perturbation of skin blood flow are summarised in Table 1. Both resting forearm blood flux and  $SO_2$  were correlated with skin temperature, all measured simultaneously at the same site (Figure 2). The relative



Accepted Article

increases in blood flux and  $SO_2$  from baseline during peak PORH were 6.7 and 2.7 fold, respectively; and after local thermal warming, 22.3 and 2.4 fold, respectively. IBH resulted in a transient fall from baseline in BF ( $8.6 \pm 3.2$  PU) and  $SO_2$  ( $41.8 \pm 13.3\%$ ) ( $n=16$ ) from resting values of 14.3 (6.4) PU and 49.5 (13.3)% ( $n=16$ ), respectively.

Examination of oxyHb and deoxyHb recorded during arterial occlusion reveals a decrease in oxyHb and increase in deoxyHb (Figure 1 inset) indicative of oxygen removal (consumption) by the tissue (6). The mean rate of oxygen desaturation measured as the initial transient in oxyHb measured over the first 60 sec of arterial occlusion was of  $-0.069 \pm 0.05$  AU.s<sup>-1</sup> ( $n=33$ ) under resting conditions.

The relationship between simultaneously recorded BF and  $SO_2$  measured at rest and during perturbation of skin blood flow is shown in Figure 3. The data are described by a one-phase association curve fit with curve equation  $SO_2 = -18.07 + 99.2*(1 - e^{-0.096*flux})$  ( $r^2=0.88$ ; 164 measurements in 50 volunteers) with an asymptote for  $SO_2$  of 84%.

Table 2 gives the Pearson correlations of resting BF and  $SO_2$  with skin temperature, BMI, age and sex. In a multivariable linear regression model resting  $SO_2$  was independently associated with resting BF (standardised  $\beta$  coefficient 0.262; 95%CI 0.092,0.900;  $p=0.017$ ), skin temperature (standardised  $\beta$  coefficient 0.503; 95%CI 1.672,4.123;  $p<0.001$ ), BMI (standardised  $\beta$  coefficient 0.298; 95%CI 0.345,1.864;  $p=0.005$ ) and age (standardised  $\beta$  coefficient -0.284; 95% CI -0.714,-0.108;  $p=0.009$ ). Skin temperature accounted for 28% of the variance in  $SO_2$  (adjusted  $r^2=0.297$ ,  $p<0.001$ ); and together BF, skin temperature, BMI and age identified 59% of the variance in  $SO_2$  (adjusted  $r^2=0.545$ ,  $p<0.001$ ).

### **Skin blood flux and oxygenation measured in the frequency domain using the combined probe**

An example of the estimated power spectra for baseline forearm BF and  $SO_2$  signals is shown in Figure 4. The most prominent frequency bands are low frequency (LF) oscillations indicative of flow motion (endothelial, neurogenic and myogenic activity). Power spectral density (PSD) estimations were initially performed over the frequency range 0.0095 – 1.6 Hz. While both BF and OXY showed periodic LF fluctuations, high frequency fluctuations attributable to cardiac and respiratory activity were absent from the OXY signals (Figure 4

and Table 3). Further PSD analysis was therefore restricted to the three lowest frequency bands. Mean relative PSD for baseline BF and SO<sub>2</sub> within these low frequency bands is shown in Figure 5. There was a significant positive correlation between the baseline BF PSD and SO<sub>2</sub> PSD contributions in each of the three low frequency bands (Figure 6).

We used frequency coherence to identify interactions between the BF and SO<sub>2</sub> signals and to determine the frequency bands where such interactions occur. The frequency coherence between the forearm BF and SO<sub>2</sub> signals measured at rest was significant over all three low frequency bands and was higher in the endothelial ( $0.57 \pm 0.20$ ) and neurogenic ( $0.56 \pm 0.15$ ) bands compared with that in the myogenic band ( $0.25 \pm 0.12$ ).

## Discussion

Tissue blood flow and oxygenation at the level of the microcirculation are two important physiological parameters indicative of tissue health. When measured in combination they provide important insight into processes that contribute to the effective oxygen delivery to metabolising tissues. There are however few devices using which these measures can be non-invasively and reliably made in a clinical setting. In this study we set out to determine the temporal relationship between blood flux and tissue oxygenation in the microvasculature of the skin of healthy individuals measured simultaneously with a novel, combined, non-invasive laser Doppler and white light reflectance spectroscopy sensor. We demonstrated that the relationship between microvascular BF and SO<sub>2</sub> measured in healthy skin at rest and during physiological perturbation of skin blood flow is best described by a one-phase association curve fit with a plateau in SO<sub>2</sub> of 84% for BF > 50 PU (achieved during maximal hyperaemia during local skin warming) and that this relationship is consistent with that described by the statement of mass balance for oxygen in the tissues (see below). We have also shown that resting skin SO<sub>2</sub> is independently associated with BF, skin temperature, BMI and age, and that these together account for 59% of the variance in SO<sub>2</sub> in our healthy cohort. Skin temperature accounted for nearly half of this variance. Our data, within the frequency domain, afford strong support for the existence and synchronicity of multiple time varying oscillations in both microvascular blood flux and tissue oxygenation in healthy skin. They have additionally revealed a significant dissociation between these oscillators, as

evidenced by their relative contribution to local flow motion activity. They suggest that the BF and SO<sub>2</sub> signals appear to be modulated by similar processes, although not at the same time, as evidenced by the relative PSD contributions to local flowmotion activity and the coherence between the BF and SO<sub>2</sub> signals across the low frequency bands.

### ***Relationship between simultaneously measured BF and OXY in the time domain***

In the time domain, absolute values of baseline and perturbed BF obtained using the combined sensor were comparable to those we and others have reported previously in healthy skin using single modality laser Doppler devices (1,2,13,42). The range of values for SO<sub>2</sub> measured using the current dual sensor are comparable with those determined in the skin and superficial muscle of healthy individuals at rest and patients with diabetes using combined light guide spectrophotometry (O2C©) (3,4,22) although direct comparison cannot be made due to the differing units of measurement and differences in sites and tissue volumes samples. They are also comparable with those measured in skeletal muscle during exercise using NIRS combined with DCS (23). The reproducibility and repeatability for resting BF and SO<sub>2</sub> measured using the combined sensor are substantial to excellent and consistent with values reported previously for single LDF sensors (1,32,51). Further, the similarity of CV for SO<sub>2</sub>, oxyHb and deoxyHb indicates that these measures of oxygenation can be used with the same level of confidence and in similar ways to laser Doppler; i.e. for inter- and intra-individual comparisons and for assessments of relative changes.

The simultaneously recorded values of BF and SO<sub>2</sub> that we report provides insight into the relationship between blood flow, oxygen saturation and consumption in the skin. The parameter of SO<sub>2</sub>, is calculated from the measures of oxyHb and deoxyHb and provides a measure of mean tissue SO<sub>2</sub> which is indicative of the balance between O<sub>2</sub> delivery and tissue O<sub>2</sub> consumption in the tissue volume sampled. The relationship between blood flow and tissue oxygenation can be described by the statement of mass balance for oxygen in the tissues, i.e. Blood flow x (Difference in O<sub>2</sub> content between arterial and venous blood) = Oxygen uptake by the tissues. If we argue that the mean SO<sub>2</sub> in cutaneous tissue is dominated by its value in the venous plexuses, the venous saturation Sv<sub>O2</sub> should be related to blood flow (F) and the tissue oxygen consumption (m<sub>O2</sub>), through the relationship:

$$S_{vO_2} = S_{aO_2} - \frac{m_{O_2}}{F \cdot [totalHb]} \quad (2)$$

where  $S_{aO_2}$  is the oxygen saturation of the arterial blood and  $[totalHb]$  is the total haemoglobin concentration ( $[deoxyHb] + [oxyHb]$ ).

Our measurements in Figure 3 appear consistent to this relationship, suggesting that venous  $SO_2$  is a reasonable approximation or at least a linear relative of mean  $SO_2$  and that  $m_{O_2}$  remains reasonably constant during the procedures that alter blood flow. Equation (2) has an equivalent form when written in terms of the deoxygenated Hb of the arterial ( $Hb_a$ ) and venous ( $Hb_v$ ) blood in the tissue, only here venous deoxygenated Hb ( $Hb_v$ ) is positively related to the reciprocal of the blood flow:

$$Hb_v = Hb_a + \frac{m_{O_2}}{F \cdot [totalHb]} \quad (3).$$

Thus, if oxygen consumption in the tissue remains constant,  $Hb_v$  should vary with the reciprocal of the product of blood flow x  $[totalHb]$ .

The negative linear relations predicted by equation (2) depend on  $m_{O_2}$  and  $[totalHb]$  remaining constant. However, examination of the output from the probe suggests that  $[totalHb]$  may change, as for example during arterial occlusion (inset Fig 1). This was possibly due to an increase in the volume of blood in the venous plexus and a small increase in haematocrit following fluid filtration. The relationship between  $SO_2$  and the reciprocal of BF ( $1/BF$ ) corrected for totalHb is consistent with that predicted above (Figure 7). The slope of this relationship ( $r^2 = 0.62$ ,  $p < 0.0001$ ) has an intercept of  $SO_2 = 78\%$  (93 paired measurements from 50 participants). We have argued above that the mean  $SO_2$  in the tissue measured by the combined probe is dominated by its value in the venules (4). This is consistent with the anatomy of the cutaneous microcirculation where most of the red cells might be expected to be found in the extensive venular plexuses of the skin (9,10). The plateau in  $SO_2$  at higher blood flows (84%) is consistent with the argument that as blood velocity increases (and hence transit times are reduced) a-v differences for  $O_2$  are reduced. That the OXY measure of  $SO_2$  at higher blood flows remains lower than that measured using pulse oximetry that excludes the influence of venous and capillary blood (arterial  $SpO_2$  of

95-97%) (12) may also be indicative of the larger contribution from blood in the venules . This is consistent with Bernjak *et al.* (4) who report median values of oxygen saturation of 47% in forearm skin using white light spectroscopy (O2C<sup>®</sup> LEA Medizintechnik Germany with a LF-2 probe, fibre separation 2 mm).

***What influences tissue oxygenation and explains the variability in SO<sub>2</sub> in our healthy cohort?***

By undertaking regression modelling, we aimed to test the assumption that resting SO<sub>2</sub> was associated with BF independently of factors that were associated with BF or SO<sub>2</sub> in univariate analyses (shown in Table 2). We found that BF, skin temperature and BMI were all independently and positively, and age independently and negatively associated with SO<sub>2</sub>. Our observation that SO<sub>2</sub> as well as BF was strongly correlated with skin temperature was not unexpected given the relationship between the two parameters and is consistent with previous findings on the effects of local warming on skin BF (2,42). It is perhaps surprising that skin temperature contributed nearly half of the variance in resting SO<sub>2</sub>, independent of BF. While there was no correlation between BF and BMI over the range of BMIs studied (median 24.3 range 17.6-32 kg.m<sup>-2</sup>), BMI was positively correlated with SO<sub>2</sub>. A relationship between BMI and a measure of oxygen extraction (average half-life of mean oxygen saturation) determined using optical reflectance spectroscopy has been reported previously in obese (BMI>29.5 kg.m<sup>-2</sup>, n=11) but not lean individuals (BMI<26.0 kg.m<sup>-2</sup>, n=8) (52). These authors proposed that the relationship in obese individuals was indicative of a reduced or less efficient oxygen extraction in obese individuals. Whether the relationship between BMI and SO<sub>2</sub> that we report in the current study in lean individuals is attributable to an altered or less efficient oxygen extraction or reduced tissue metabolism with increasing BMI has yet to be fully explored.

It has been suggested that the early transient slope of oxygen desaturation during arterial occlusion measured in muscle using NIRS is indicative of tissue oxygen consumption (6,23,31). In the current study in skin, the early transient in oxyHb measured during the first 60 seconds of arterial occlusion was taken as a coefficient of tissue oxygen consumption. As might be anticipated we found that the oxyHb slope coefficient (indicative of the utilisation

of oxygen by the skin) was correlated with forearm temperature ( $r^2=0.21$ ,  $p=0.007$ ). Further studies are required to understand better the dynamics of the oxyHb and deoxyHb transients studied with white light reflectance spectroscopy and their potential in the evaluation of haemodynamic and metabolic parameters in the skin.

### ***Relationship between simultaneously measured BF and SO<sub>2</sub> in the frequency domain***

In the current study we initially estimated the PSD of the BF and SO<sub>2</sub> signals across five previously defined frequency bands (48). We found that both BF and SO<sub>2</sub> oscillate over broad, generally similar frequency ranges of 0.0095-0.15 Hz. Our data reveal differences in the absolute power and oscillatory characteristics of the simultaneously recorded BF and SO<sub>2</sub> signals; with a higher total power and relative contribution from the endothelial band and negligible respiratory and cardiogenic oscillations in the SO<sub>2</sub> signal compared with that in the BF signal. The relative energy content of the five bands within the resting BF trace was similar to that reported previously in healthy human skin (8) but showed differing trends in relative PSD in the 5 bands to those reported previously by us and other groups (13,28,47). This is perhaps not surprising considering the temporal variability in LDF and the limited number of individuals studied. The relatively small contribution of respiratory and cardiac activities to the SO<sub>2</sub> signal is similar to that observed in the brain using NIRS (44) and skin using optical reflectance spectroscopy (4,52). Together these data suggest that SO<sub>2</sub> dynamics have a longer time constant than BF measured using LDF. While our understanding of the mechanisms regulating microvascular blood flow and tissue oxygenation is far from complete, PSD analysis of simultaneously recorded BF and SO<sub>2</sub> suggests differing flow motion and vasomotor control mechanisms with some common features. However, PSD analysis does not reveal information about concordancy of these oscillations and so we investigated this using frequency coherence to provide an additional characteristic of the dynamics of the studied signals. Considering these two signals have been recorded simultaneously and have a common source (RBC), we would expect a degree of similarity in spontaneous oscillations. Our findings demonstrate considerable frequency coherence within the endothelial and neurogenic bands and suggest the endothelial and neurogenic activities of microvascular control are modulated in a similar manner in BF and SO<sub>2</sub>. These findings support and extend those of Bernjak *et al.* (4) who use the wavelet transform and phase coherence to analyse the BF-SO<sub>2</sub> relationship measured with O2C while we have

considered data collected using the combined Moor OXY and LDF probe and presented results using FFT analysis. What is striking is the degree of agreement between these two independent studies using different but broadly complimentary measurement and analysis methods.

Our findings are also consistent with those of Thorn *et al.* (52) who demonstrated the influence of vasomotion on oxygen extraction and specifically that related to endothelial activity. The concordancy of the neurogenic flow motion component in the skin microvascular BF and tissue  $SO_2$  signals that we observe is also consistent with the highly correlated sympathetically-mediated changes in forearm muscle oxygenation (NIRS) and brachial artery blood flow (Doppler ultrasound) observed by Fadel *et al.* (19) in healthy humans.

#### ***Strengths and Limitations of our study***

A major strength of our study is that through the use of a combined non-invasive probe that simultaneously measures skin microvascular blood flux, tissue haemoglobin concentration (oxyHb, deoxyHb and totalHb), oxygen saturation ( $SO_2$ ) and temperature at the same skin site we have been able to test assumptions around the relationship between microvascular blood flow and tissue oxygenation and utilization in the skin. Secondly, we have analysed long data sets of continuously acquired signals to investigate the synchronicity of the rhythms in these multiple signals and their association with local flow motion and vasomotor control. Finally, our study was conducted in 50 healthy human volunteers using well characterised physiological perturbations in peripheral blood flow. The data obtained from these healthy individuals provide a reference against which to investigate the utility of the combined sensor and the relationship between microvascular perfusion and tissue haemoglobin and oxygen saturation in a clinical setting, in patients at risk of, or with, microvascular impairment.

Our study may also have limitations. It is likely that the volume of tissue sampled using the LDF and OXY techniques is different. From a purely geometrical perspective the depth sampled by the OXY assessment should be greater by the ratio of the optical fibre

Accepted Article

separations (1 mm for white light OXY, 0.5 mm for LDF). However, the LDF signal is computed from the frequency-weighted power spectrum. The larger elements of the microvascular bed lie deeper in the dermis and these contain faster moving blood flow so the LD frequency-weighting will tend to increase the sampling depth beyond what might be expected from a purely geometric perspective. The OXY signal is not frequency weighted; therefore the tissue volume sampled by this technique is determined purely from geometric/light diffusion considerations. However, with the assumption that OXY is dominated by venous flow and LDF is dominated by arterial flow (due to frequency-weighting), depth and volume may be similar but the signal origins within this volume may differ. It should also be recognized that BF, oxyHb, deoxyHb and SO<sub>2</sub> are distributed heterogeneously along the light path and so the output from the probe represents an average through the sampled volume of tissue. Further, the relative contribution from arterioles, capillaries and venules to SO<sub>2</sub> will vary depending on the distribution of blood between these vascular compartments. This may go some way to accounting for the differences in reported oxygen saturation measured using different spectroscopic devices that sample to different tissue depths and differentially influence of venous and capillary blood (4,12,52).

Many previous studies in which frequency analysis of the LDF signal has been reported, present data as relative energy of the scalogram expressed in % (25) or as relative spectral amplitude or PSD (6,13,2019,39). Thus, it is difficult to compare results directly. We selected 10 min of artefact-free signal for analysis in the frequency domain. Ten minutes of data covers six cycles of the 0.01 Hz band attributed to the endothelium and, despite potentially relatively poor low frequency resolution compared to the other frequency bands considered, was sufficient to ascribe relative power contributions to modulating frequency bands. It would be possible to enhance the resolution by employing longer measurement periods. Averaging of individual scalograms across the volunteers may obscure both some of the time-varying frequencies and PSD over time, particularly as the higher frequency activities are present in one data set (BF) and not the other (SO<sub>2</sub>). Similarly, averaging the coherence from the group may obscure the variability present in the individuals. These issues will need to be addressed in future studies if the consequences of changes in rhythmical flow motion on tissue perfusion and oxygenation under pathophysiological



Accepted Article

conditions are to be investigated.

Finally, we have undertaken our study in the skin microvasculature, the main function of which is in thermoregulation and protection from the external environment and which may thus not be representative of microvascular beds in other tissues. While the concept of skin microcirculation as a peripheral index or surrogate of vascular health remains contentious, we would argue from our own investigations and those of others (18,41) that monitoring local tissue perfusion in combination with tissue oxygen parameters, could provide an early indicator of compromised tissue function and a fast and effective tool to augment the diagnosis, treatment and management of conditions across a number of clinical specialities in which microvascular dysfunction plays a role.

### **Perspectives**

The real-time collection of robust measures of microvascular blood flow and blood oxygenation parameters can provide novel information of the relationship between microvascular perfusion and tissue oxygenation in human skin in vivo. We have used a novel combined non-invasive sensor to determine the dynamics of microvascular blood flow and tissue oxygenation parameters in a cohort of 50 healthy human volunteers. We have defined the relationship between skin microvascular blood flow and oxygenation over a wide range of physiological flows. Further, we have shown the synchronicity of the rhythms in these multiple, continuously acquired signals and their association with local flow motion and mechanisms of vasomotor control. Together these findings provide a platform from which to investigate microvascular impairment in the skin.

### **Acknowledgements**

We thank Keith McCormick for his assistance in volunteer recruitment. This study was supported by the NIHR/WellcomeTrust Southampton Clinical Research Facility. KK is in receipt of an EPSRC CASE studentship.

## Declaration

RG is an employee of Moor Instruments Ltd.

**Table 1** Skin blood flux (BF) and tissue oxygenation (OXY) measured in 50 healthy participants at baseline; during arterial occlusion (180 mmHg, 3 min); at peak post occlusive reactive hyperaemia (PORH); and after local warming (43°C, 20 min). BF was recorded in arbitrary perfusion units (PU) and SO<sub>2</sub> in per cent (%) and is derived from the measures of oxygenated (oxyHb) and deoxygenated haemoglobin (deoxyHb) (measured in arbitrary units, AU).

|                  | <b>Blood Flux (PU)</b> | <b>SO<sub>2</sub> (%)</b> | <b>oxyHb (AU)</b> | <b>deoxyHb (AU)</b> |
|------------------|------------------------|---------------------------|-------------------|---------------------|
|                  | <b>mean (SD)</b>       | <b>mean (SD)</b>          | <b>mean (SD)</b>  | <b>mean (SD)</b>    |
| <b>Resting</b>   | 11.8 (6.1)             | 44.6 (12.4)               | 6.2 (3.0)         | 8.2 (3.6)           |
| <b>Occluded</b>  | 3.2 (0.6)              | 2.4 (3.7)                 | 0.4 (0.6)         | 20.2 (8.6)          |
| <b>Peak PORH</b> | 77.7 (34.4)            | 81.4 (5.9)                | 23.3 (7.8)        | 5.7 (2.6)           |
| <b>Warmed</b>    | 193.0 (80.3)           | 83.0 (3.7)                | 34.9 (8.4)        | 7.5 (3.2)           |

**Table 2** Pearson correlations between microvascular skin blood flux (BF), oxygenation (SO<sub>2</sub>), skin temperature measured at rest and cohort phenotype (n= 50).

|                                | <b>BF</b> |                | <b>SO<sub>2</sub></b> |                |
|--------------------------------|-----------|----------------|-----------------------|----------------|
|                                | <b>r</b>  | <b>p value</b> | <b>r</b>              | <b>p value</b> |
| <b>SO<sub>2</sub> (%)</b>      | 0.456     | 0.001          |                       |                |
| <b>Skin temperature (°C)</b>   | 0.343     | 0.017          | 0.549                 | 0.0001         |
| <b>BMI (kg.m<sup>-2</sup>)</b> | 0.093     | 0.269          | 0.374                 | 0.005          |
| <b>Age (y)</b>                 | -0.136    | 0.360          | -0.284                | 0.028          |

Sex 0.119 0.182 0.098 0.258

**Table 3** Median (IQR) of power in simultaneously recorded BF and SO<sub>2</sub> measured at the same skin site. Total power was evaluated in the frequency range (0.0095-1.6 Hz) and divided into frequency intervals corresponding to endothelial (0.0095-0.02 Hz), neurogenic (0.02-0.06 Hz), myogenic (0.06-0.15 Hz), respiratory (0.15-0.4 Hz) and cardiogenic (0.4-1.6 Hz). Spectral density was estimated by Welch's method of Fourier transform with Hanning window size of 200s and 50% overlap between windows. Data are from 31 healthy individuals. \* p< 0.0001.

| Frequency band | BF (PU <sup>2</sup> ), median (IQR) | SO <sub>2</sub> (AU <sup>2</sup> ), median (IQR) |
|----------------|-------------------------------------|--|
| Endothelial    | 0.38 (0.14-1.01)                    | 5.65 (2.53-13.56)*                               |
| Neurogenic     | 0.88 (0.54-1.70)                    | 6.61 (4.07-13.47)*                               |
| Myogenic       | 0.56 (0.27-0.98)                    | 0.87 (0.33-1.51)                                 |
| Respiratory    | 0.40 (0.15-0.74)                    | 0.04 (0.02-0.05)*                                |
| Cardiogenic    | 0.74 (0.36-1.69)                    | 0.06 (0.05-0.10)*                                |
| Total          | 3.16 (1.84-5.86)                    | 13.95 (8.85-27.06)*                              |

#### References

1. Agarwal SC, Allen J, Murray A & Purcell IF. Comparative reproducibility of dermal microvascular blood flow changes in response to acetylcholine iontophoresis, hyperthermia and reactive hyperaemia. *Physiol Meas* 31: 1-11, 2010
2. Avery MR, Voegeli D, Byrne CD, Simpson DM & Clough GF. Age and cigarette smoking

are independently associated with the cutaneous vascular response to local warming. *Microcirculation* 16: 725-734, 2009.

3. Beckert S, Witte MB, Königsrainer A & Coerper S. The Impact of the Micro-Lightguide O2C for the Quantification of Tissue Ischemia in Diabetic Foot Ulcers. *Diabetes Care* 27: 2863-2867, 2004.
4. Bernjak A, Stefanovska A, McClintock PVE, Owen-Lynch PJ, Clarkson PBM. Coherence between fluctuations in blood flow and oxygen saturation. *Fluctuations and Noise Letters* 11:1240013-1 – 1240013-12, 2012.
5. Bland M. An Introduction to Medical Statistics. Oxford University Press, London. 2000
6. Boas DA & Franceschini MA. Haemoglobin oxygen saturation as a biomarker: the problem and a solution. *Philos Trans A Math Phys Eng Sci* 369: 4407-4424, 2011
7. Bonner R & Nossal R. Model for laser Doppler measurements of blood flow in tissue. *Appl Opt* 20: 2097-2107, 1981.
8. Bracic M & Stefanovska A. Wavelet-based analysis of human blood-flow dynamics. *Bull Math Biol* 60: 919-935, 1998.
9. Braverman IM. The cutaneous microcirculation: ultrastructure and microanatomical organization. *Microcirculation* 4: 329-340, 1997.
10. Braverman IM. The cutaneous microcirculation. *J Invest Dermatol Symp Proc* 5: 3-9, 2000.
11. Challis RE & Kitney RI. Biomedical signal processing (in four parts). *Med Biol Eng Comput* 29: 225-241, 1991.
12. Chan ED, Chan MM, Chan MM. Pulse oximetry: understanding its basic principles facilitates appreciation of its limitations. *Respir Med* 107: 789-799, 2013
13. Clough G, Chipperfield A, Byrne C, de Mul F & Gush R. Evaluation of a new high power, wide separation laser Doppler probe: potential measurement of deeper tissue blood flow. *Microvasc Res* 78: 155-161, 2009.
14. Clough GF, L'Esperance V, Turzyniecka M, Walter L, Chipperfield AJ, Gamble J, Krentz AJ

& Byrne CD. Functional dilator capacity is independently associated with insulin sensitivity and age in central obesity and is not improved by high dose statin treatment. *Microcirculation* 18: 74-84, 2011.

15. Czernichow S, Greenfield JR, Galan P, Jellouli F, Safar ME, Blacher J, Hercberg S & Levy BI. Macrovascular and microvascular dysfunction in the metabolic syndrome. *Hypertens Res* 33: 293-297, 2010.
16. Davis SL, Fadel PJ, Cui J, Thomas GD, Crandall CG. Skin blood flow influences near-infrared spectroscopy-derived measurements of tissue oxygenation during heat stress. *J Appl Physiol*: 221-224, 2006.
17. De Blasi RA, Ferrari M, Natali A, Conti G, Mega A, Gasparetto A. Noninvasive measurement of forearm blood flow and oxygen consumption by near-infrared spectroscopy. *J Appl Physiol* 76: 1388-93, 1994.
18. De Boer MP, Meijer RI, Wijnstok NJ, Jonk AM, Houben AJ, Stehouwer CD, Smulders YM, Eringa EC & Serné EH. Microvascular Dysfunction: A Potential Mechanism in the Pathogenesis of Obesity-associated Insulin Resistance and Hypertension. *Microcirculation* 19: 5-18, 2012.
19. Fadel PJ, Keller DM, Watanabe H, Raven PB, Thomas GD. Noninvasive assessment of sympathetic vasoconstriction in human and rodent skeletal muscle using near-infrared spectroscopy and Doppler ultrasound. *J Appl Physiol* 96: 1323-1330, 2004.
20. Fedorovich AA. Non-invasive evaluation of vasomotor and metabolic functions of microvascular endothelium in human skin. *Microvasc Res* 84: 86-93, 2012.
21. Ferrari M, Muthalib M, Quaresima V. The use of near-infrared spectroscopy in understanding skeletal muscle physiology: recent developments. *Philos Trans A Math Phys Eng Sci* 369:4577-4590, 2011.
22. Forst T, Hohberg C, Tarakci E, Forst S, Kann P & Pfutzner A. Reliability of lightguide spectrophotometry (O2C) for the investigation of skin tissue microvascular blood flow and tissue oxygen supply in diabetic and nondiabetic subjects. *J Diabetes Sci Technol* 2: 1151-1156, 2008.

23. Gómez H, Torres A, Polanco P, Kim H, Zenker S, Puyana J & Pinsky M. Use of non-invasive NIRS during a vascular occlusion test to assess dynamic tissue O<sub>2</sub> saturation response. *Intensive Care Med* 34,:1600-1607, 2008.
24. Gurley K, Shang Y & Yu G. Noninvasive optical quantification of absolute blood flow, blood oxygenation, and oxygen consumption rate in exercising skeletal muscle. *J Biomed Opt* 17: 075010, 2012.
25. Humeau A, Chapeau-Blondeau Fo, Rousseau D, Rousseau P, Trzepizur W & Abraham P. Multifractality, sample entropy, and wavelet analyses for age-related changes in the peripheral cardiovascular system: Preliminary results. *Med Physics* 35: 717-723, 2008.
26. Khan F, Green FC, Forsyth JS, Greene SA, Morris AD, Belch JJ. Impaired microvascular function in normal children: effects of adiposity and poor glucose handling. *J Physiol* 551:705-11, 2003.
27. Kvandal P, Landsverk SA, Bernjak A, Stefanovska A, Kvernmo HD & Kirkebøen KA. Low-frequency oscillations of the laser Doppler perfusion signal in human skin. *Microvasc Res* 72: 120-127, 2006.
28. Kvernmo H, Stefanovska A & Kirkebøen K. Enhanced endothelial activity reflected in cutaneous blood flow oscillations of athletes. *Eur J Appl Physiol* 90: 16-22, 2003.
29. Kvernmo HD, Stefanovska A, Kirkebøen KA & Kvernebo K. Oscillations in the Human Cutaneous Blood Perfusion Signal Modified by Endothelium-Dependent and Endothelium-Independent Vasodilators. *Microvasc Res* 57: 298-309, 1999.
30. L'Esperance VS, Cox SE, Simpson D, Gill C, Makani J, Soka D, Mgaya J, Kirkham FJ & Clough GF. Peripheral vascular response to inspiratory breath hold in paediatric homozygous sickle cell disease. *Exp Physiol* 98: 49-56, 2013.
31. Lipcsey M, Woinarski N & Bellomo R. Near infrared spectroscopy (NIRS) of the thenar eminence in anesthesia and intensive care. *Ann Intensive Care* 2: 11, 2012.
32. Liu H, Kohl-Bareis M, Huang X. Design of a tissue oxygenation monitor and verification on human skin. In *Clinical and Biomedical Spectroscopy and Imaging II*, N. Ramanujam

and J. Popp, eds., Vol. 8087 of Proceedings of SPIE-OSA Biomedical Optics (Optical Society of America, 2011), paper 80871Y.

33. Minson CT. Thermal provocation to evaluate microvascular reactivity in human skin. *J Appl Physiol* 109: 1239-1246, 2010.
34. Nilsson GE, Tenland T & Oberg PA. A New Instrument for Continuous Measurement of Tissue Blood Flow by Light Beating Spectroscopy. *IEEE Trans Biomed Eng* 27: 12-19, 1980.
35. Pachauri NaM, DK. Phase Synchronization and Coherence Analysis between ECG & Arterial Blood Pressure. *Int J Comp Appl* 44: 27-80, 2012.
36. Park C, Bathula R, Shore AC, Tillin T, Strain WD, Chaturvedi N, Hughes AD. Impaired post-ischaemic microvascular hyperaemia in Indian Asians is unexplained by diabetes or other cardiovascular risk factors. *Atherosclerosis* 221:503-7, 2012.
37. Pereda E, Quiroga RQ & Bhattacharya J. Nonlinear multivariate analysis of neurophysiological signals. *Prog Neurobiol* 77: 1-37, 2005.
38. Phillip D, Iversen HK, Schytz HW, Selb J, Boas DA, Ashina M. Altered Low Frequency Oscillations of Cortical Vessels in Patients with Cerebrovascular Occlusive Disease - A NIRS Study. *Front Neurol* 4: 204, 2013.
39. Rossi M, Bradbury A, Magagna A, Pesce M, Taddei S & Stefanovska A. Investigation of skin vasoreactivity and blood flow oscillations in hypertensive patients: effect of short-term antihypertensive treatment. *J Hypertens* 29: 1569-1576, 2011.
40. Rossi M, Carpi A, Di Maria C, Galetta F & Santoro G. Spectral analysis of laser Doppler skin blood flow oscillations in human essential arterial hypertension. *Microvasc Res* 72; 34-41, 2006.
41. Roustit M & Cracowski JL. Non-invasive assessment of skin microvascular function in humans: an insight into methods. *Microcirculation* 19: 47-64, 2012.
42. Roustit M, Maggi F, Isnard S, Hellmann M, Bakken B & Cracowski JL. Reproducibility of a local cooling test to assess microvascular function in human skin. *Microvasc Res* 79: 34-39, 2010.

43. Sakr Y. Techniques to assess tissue oxygenation in the clinical setting. *Transfus Apher Sci* 43: 79-94, 2010.
44. Schroeter ML, Schmiedel O & von Cramon DY. Spontaneous Low-Frequency Oscillations Decline in the Aging Brain. *J Cereb Blood Flow Metab* 24: 1183-1191, 2004.
45. Shang Y, Gurley K, Symons B, Long D, Srikuea R, Crofford L, Peterson C & Yu G. Noninvasive optical characterization of muscle blood flow, oxygenation, and metabolism in women with fibromyalgia. *Arthritis Res Therapy* 14: 1-12, 2012.
46. Simpson DM, BoteroRosas DA & Infantosi AFC. Estimation of coherence between blood flow and spontaneous EEG activity in neonates. *IEEE Trans Biomed Eng* 52: 852-858, 2005.
47. Soderstrom T, Stefanovska A, Veber M & Svensson H. Involvement of sympathetic nerve activity in skin blood flow oscillations in humans. *Am J Physiol Heart Circ Physiol* 284: H1638-H1646, 2003.
48. Stefanovska A, Bracic M & Kvernmo HD. Wavelet analysis of oscillations in the peripheral blood circulation measured by laser Doppler technique. *IEEE Trans Biomed Eng* 46: 1230-1239, 1999.
49. Stiefel P, Moreno-Luna R, Vallejo-Vaz AJ, Beltran LM, Costa A, Gomez L, Ordonez A & Villar J. Which parameter is better to define endothelial dysfunction in a test of postocclusive hyperemia measured by laser-Doppler flowmetry? *Coron Artery Dis* 23: 57-61, 2012.
50. Strain WD, Adingupu DD & Shore AC. Microcirculation on a large scale: techniques, tactics and relevance of studying the microcirculation in larger population samples. *Microcirculation* 19: 37-46, 2012.
51. Svalestad J, Hellem S, Vaagbø G, Irgens A, Thorsen E. Reproducibility of transcutaneous oximetry and laser Doppler flowmetry in facial skin and gingival tissue. *Microvasc Res* 79: 29-33, 2010.
52. Thorn CE, Kyte H, Slaff DW & Shore AC. An association between vasomotion and oxygen



extraction. *Am J Physiol Heart Circ Physiol* 301: H442-H449, 2011.

**Figure 1.** Simultaneous outputs from the combined BF+OXY+temperature probe recorded in the skin at the ventral forearm at rest and during the response to arterial occlusion (180 mmHg, 3 min). Main panel A) laser Doppler blood flux (arbitrary perfusion units; PU); B) tissue oxygenation ( $SO_2$ , %) where  $SO_2 = (\text{oxyHb}/\text{totalHb}) \times 100 \%$ ; C) oxygenated (oxyHb), deoxygenated haemoglobin (deoxyHb) and total haemoglobin (totalHb = oxyHb + deoxyHb) in arbitrary units (AU); D) occlusion cuff pressure (mmHg). Inset shows time expanded recording during the first 60 seconds following cuff inflation (arrow).

**Figure 2.** Relationship between (A) resting blood flux (BF) and (B) tissue oxygenation ( $SO_2$ ) and skin temperature recorded simultaneously in the skin of the forearm using a combined laser Doppler, tissue oxygenation and temperature probe (CP1T-1000, Moor Instruments) in 50 healthy volunteers. The slope of the linear regression was (A)  $r^2=0.12$ ,  $p=0.0143$ , (B)  $r^2=0.27$ ,  $p=0.0001$ ).

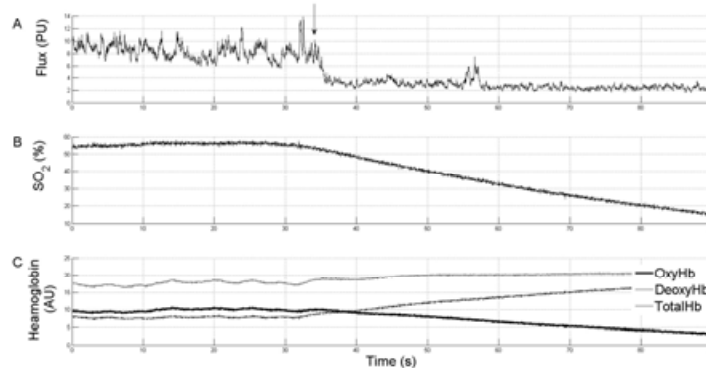
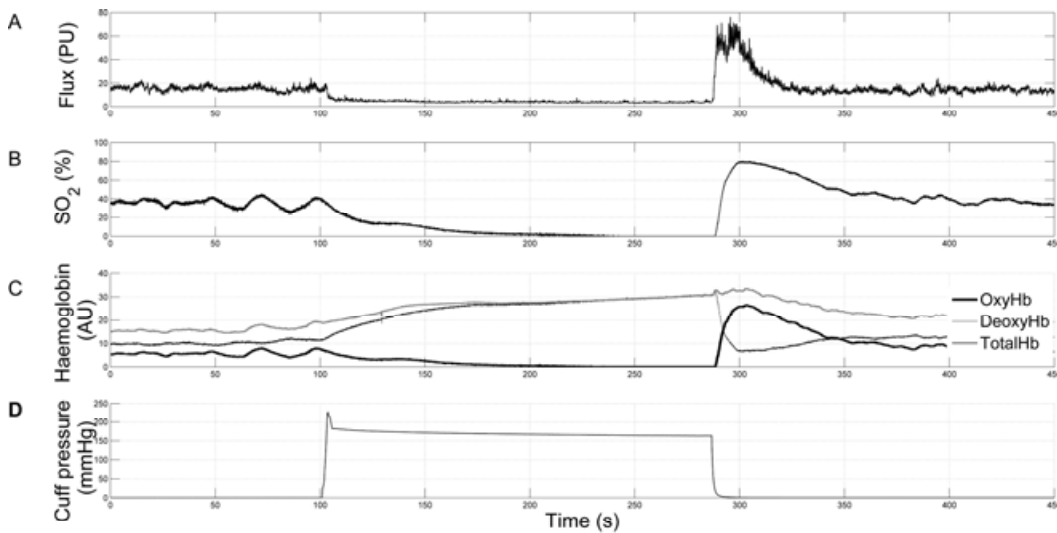
**Figure 3.** Relationship between forearm skin blood flux (BF) and tissue oxygenation ( $SO_2$ ) for simultaneously recorded values of BF and  $SO_2$  at rest (●) and during arterial occlusion (180 mmHg 3 min) (■); peak post occlusive reactive hyperaemia (▲); local thermal warming (43°C 20 min) (▼); and during the vasoconstrictor response to deep inspiratory breath hold (IBH) (◆). Data are from  $n=50$  healthy individuals. (A) The relationship between BF and  $SO_2$  in the time domain measured during these manoeuvres was established using a one-phase association  $SO_2 = -18.07 + 99.2 \cdot (1 - e^{-0.096 \cdot \text{flux}})$  ( $r^2=0.88$ ; 164 measurements in 50 volunteers). (B) Inset expanded relationship for BF up to 50 PU.

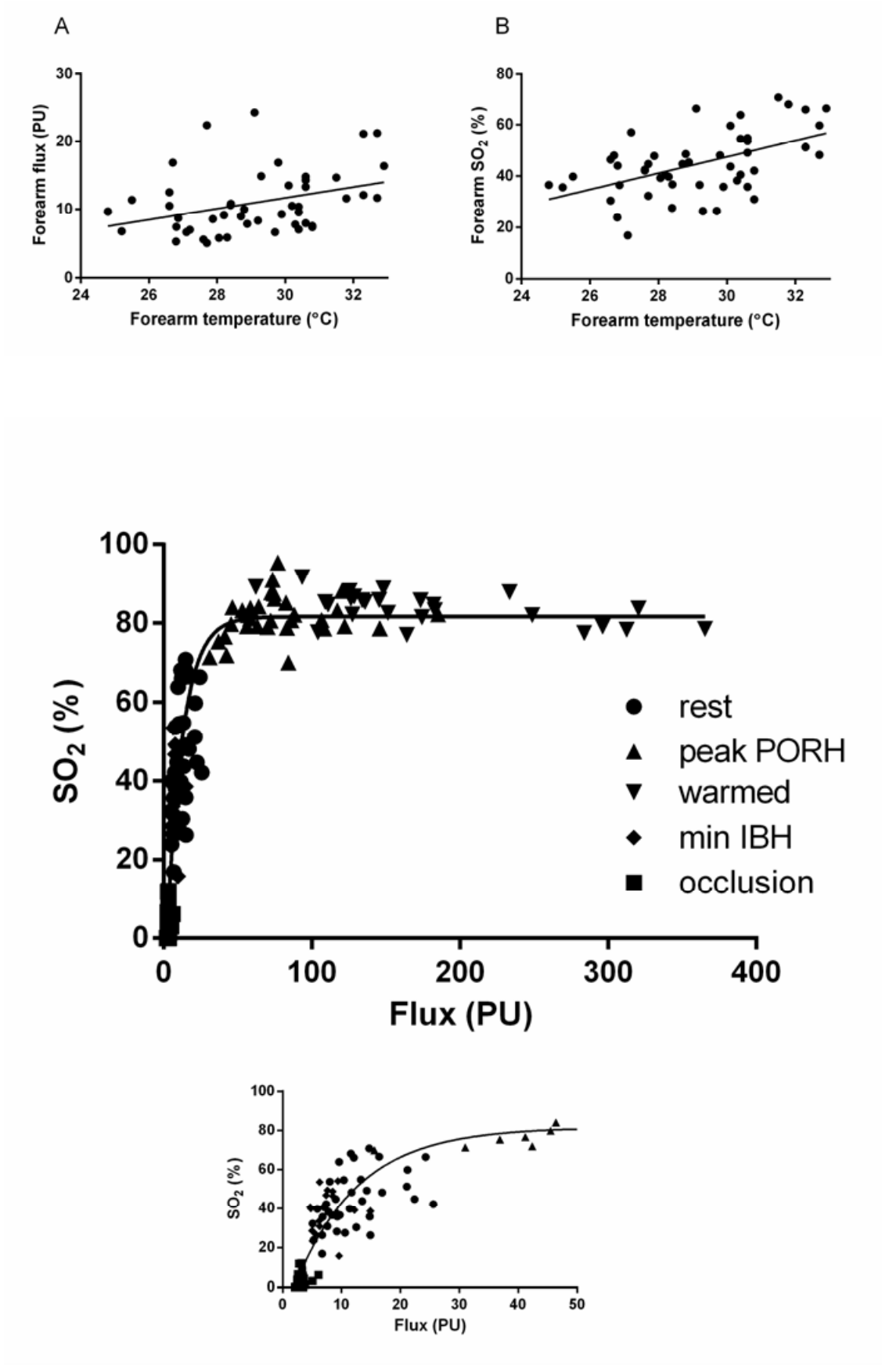
**Figure 4.** An example of (A) baseline forearm blood flux (BF) and (B) tissue oxygenation ( $SO_2$ ) and (C) their power spectrum estimated for frequency range 0.0095-2 Hz divided into 5 frequency bands. Power spectral density (PSD) was measured across five spectral bands.

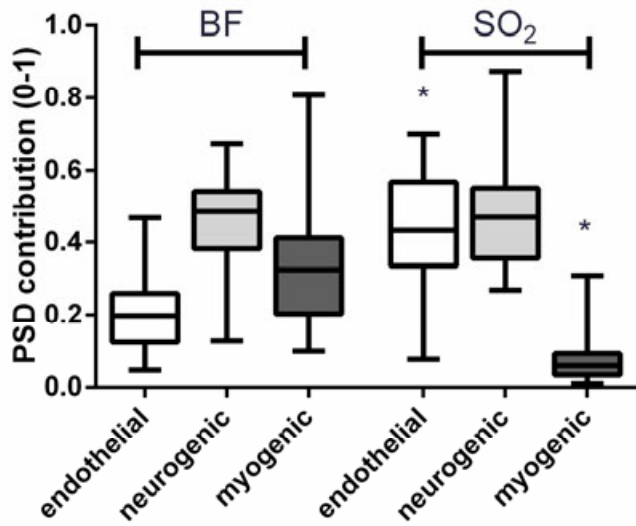
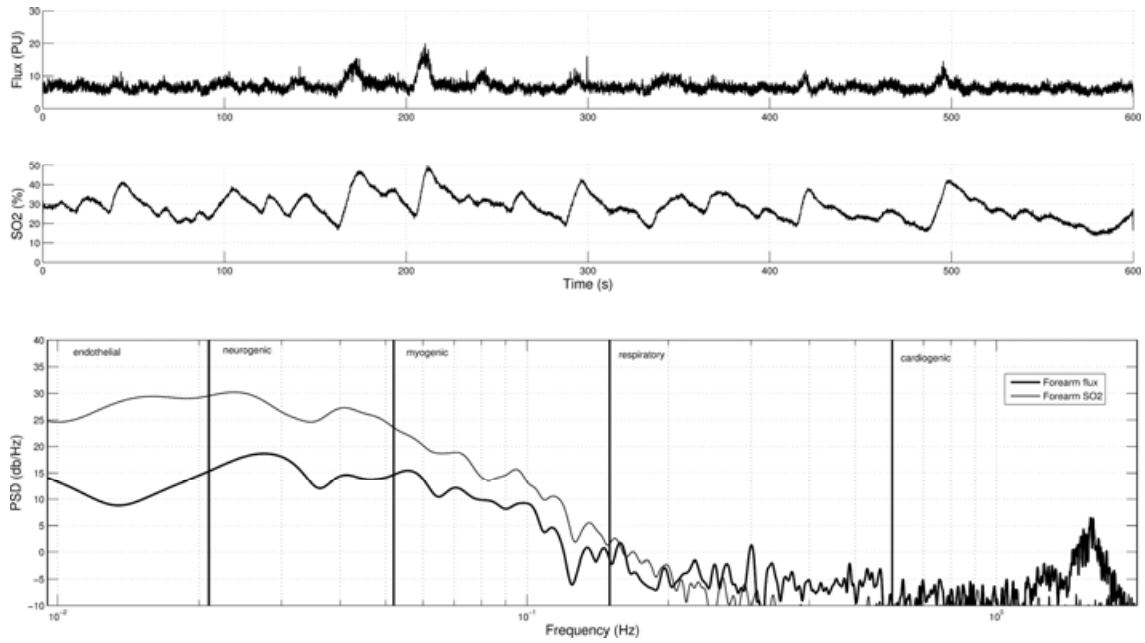
**Figure 5.** Power spectral density (PSD) contribution across three frequency bands (endothelial 0.0095-0.02 Hz, neurogenic 0.02-0.06 Hz, myogenic 0.06-0.15 Hz) expressed relative to total power spectral density in the frequency range 0.0095-0.15 Hz in simultaneously recorded BF and  $SO_2$  signals measured at the same skin site. Data shown are median, IQR and range for  $n=31$ .  $*p < 0.001$  BF vs  $SO_2$ . (Absolute and total powers from which these data are calculated are shown in Table 3).

**Figure 6.** Linear regression of blood flux (BF) and tissue oxygenation (SO<sub>2</sub>) power spectral densities (PSD) measured simultaneously at the same skin site. Frequency intervals corresponding to (A) endothelial (0.0095-0.02 Hz), (B) neurogenic (0.02-0.06 Hz), (C) myogenic (0.06-0.15 Hz) activity. Data are for n= 31 healthy individuals. All three correlations between PSD of SO<sub>2</sub> and BF signals are significant (endothelial band slope=0.49, r<sup>2</sup>=0.13, p=0.04; neurogenic band slope=0.36, r<sup>2</sup>=0.13, p=0.04; myogenic band slope=0.34 r<sup>2</sup>=0.68, p<0.0001).

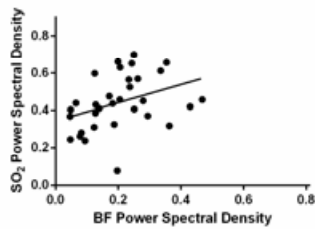
**Figure 7.** Relationship between the reciprocal of forearm skin blood flux (BF) corrected for totalHb and tissue oxygenation (SO<sub>2</sub>) for the simultaneously recorded values of BF and SO<sub>2</sub> in healthy volunteers for BF>5 PU. (r<sup>2</sup> = 0.62, p < 0.0001).



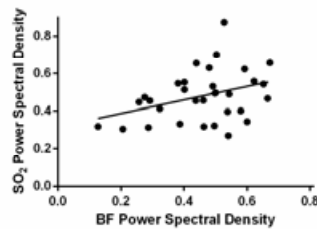




A endothelial band



B neurogenic band



C myogenic band

